Published in the Proceedings of the 16th International Aluminum Alloys Conference (ICAA16) 2018
ISBN: 978-1-926872-41-4
by the Canadian Institute of Mining, Metallurgy & Petroleum

UNDERSTANDING THE ROLE OF Cu ON THE WORK-HARDENING AND STRAIN-RATE SENSITIVITY OF 6XXX Al ALLOYS

[*]M. Langille[1, 2], B. J. Diak[3], F. De Geuser[1], A. Deschamps[1], and G. Guiglionda[2]

[1] Univ. Grenoble Alpes, CNRS, Grenoble INP, SIMaP
F-38000 Grenoble, France
([*]Corresponding author: michael.langille@simap.grenoble-inp.fr)
[2] Constellium Technology Center (C-TEC)

Voreppe, France
[3] Mechanical and Materials Engineering, Queen's University
Kingston, ON, Canada

ABSTRACT

Increased demand for light-weighting in passenger vehicles has created a need for strong, light, ductile materials to be used in body-in-white applications. The AA6xxx-series of aluminum alloys are suitable candidates meeting most requirements but can fall short of the formability demands of designers, necessitating an understanding of what controls the formability in this alloy series. This work examines the effect of copper alloying in AA6xxx on the pre-ageing and natural ageing responses of the microstructure and mechanical properties. The changes in microstructure observed by differential scanning calorimetry and hardness testing are related to the work-hardening and strain-rate sensitivity parameters for these alloys measured by tensile testing. An observed asymmetry in the measured strain-rate sensitivity associated with increasing versus decreasing strain rate changes suggests that a different mechanism operates for the two conditions. It is postulated how this asymmetry in strain-rate sensitivity will impact the necking and ductility behaviour of these alloys.

KEYWORDS

Al-Mg-Si-Cu, Clusters, Ductility, Natural ageing, Strain rate sensitivity, Tensile test, Work hardening

INTRODUCTION

The widespread use of AA6xxx series alloys in the form of sheets has provided the need for a more thorough understanding of the complex interactions between composition, processing, resulting microstructure and ultimately, the mechanical properties of the alloys. Conventional industrial practices involve the production of rolled AA6xxx sheet (typically 1 mm thick) to be used for body-in-white (BIW) applications for auto body panels (Hirsch, 2004, 2014). The final metallurgical step prior to the shipment of these panels to manufacturers involves a solution heat treatment (SHT) reverting the ageing products of the alloys into solid solution and the product is then shipped to the customer. During this shipping time and while sheets are waiting to be used, the natural ageing (NA) process occurs whereby the strength of the alloys increases resulting in reduced formability. This can result in a product that is unable to meet the formability demands of the automotive manufacturer. As a result, industry has moved towards performing pre-ageing (PA) treatments to prolong the "shelf-life" of the material prior to it having insufficient formability. Once formed into BIW panels, the parts are then painted and subsequently undergo the paint curing heat treatment which consists of a short period of time at medium temperature, typically 20 minutes at 170–190°C. This short artificial ageing (AA) treatment, known as the paint bake (PB), provides additional strength and improved dent resistance for the material, but reduced formability. The PB result is strongly dependent on the PA treatment performed prior to the forming operation. Furthermore, the addition of copper (Cu) to a base Al-Mg-Si composition is known to increase the alloy's strength. The goal of this work is to study the effect of Cu on strength, strain hardening, and strain-rate sensitivity (SRS) of these alloys, to understand the strength-formability compromise, for two separate heat treatment schedules; one including and one excluding the PA treatment, both followed by NA.

Natural and Pre-Ageing of AA6xxx Series Alloys

Age-hardenable alloys are named as such due to the increased strength obtained over time due to the diffusion of solute atoms within the metal resulting in the formation of dislocation obstacles, either clusters or precipitates. The obstacle types are largely dependent on the composition and both the ageing time and temperature. Generally, the solid solution, cluster, and precipitate sequence for a solutionized and quenched AA6xxx series alloy follows:

$$SSSS \rightarrow \text{cluster type i,ii} \rightarrow \beta'' \rightarrow \beta', Q' \rightarrow \beta, Q$$

The supersaturated solid solution (SSSS) decomposes into either type i or type ii clusters depending on the process temperature being below or above 70°C, respectively, and then the clusters evolve into precipitates if sufficient thermal energy is provided (ageing temperature) in order to overcome the activation barrier for precipitate formation. The driving force for clustering and precipitation is the reduction of Gibbs free energy within the alloy system. It was observed by Hono et al. (Murayama & Hono, 1999; Murayama, Hono, Miao, & Laughlin, 2001) that the clusters types i and ii have relatively lower, and higher (Cu + Mg)/Si ratios, respectively. The β", β' and β precipitates dominate the alloys during conventional thermal treatments having little to no Cu, being primarily Mg-Si based where the Mg component dominates up to Mg_2Si for β. When Cu is added, the appearance of Q′ and Q, precipitates have been found (Esmaeili, Wang, Lloyd, & Poole, 2003; Wenner, Marioara, Andersen, & Holmestad, 2012) with some Cu taking place of the Mg such that the (Cu + Mg)/Si ratio of these precipitates are greater than unity. Since the higher-order precipitates (β", β', β, Q, etc.) typically have a Mg/Si ratio greater than one, having clusters with a stoichiometric ratio close to this value promotes their formation during the PB cycle. In the cases when the cluster stoichiometric ratio is further from that of the precipitate composition, a deteriorated PB response was reported (Tao et al., 2015). The "negative natural ageing effect" of this alloy series is found when prolonged NA reduces the subsequent PB response, resulting in a body panel that is too soft. Cu additions or PA processes can promote the formation of type ii clusters, or clusters with (Cu + Mg)/Si ratios closer to, or greater than one, thus reducing the thermodynamic barrier to precipitate formation resulting in an improved PB response and elimination of the negative natural ageing effect (Kim & Sato, 2011). However, strength is not the only consideration in sheet alloys; the effects of Cu and heat treatment on the ductility, strain-rate sensitivity, and formability must also be considered, being critical to the forming processing taking place before the PB process.

Conventionally, the Considère criterion has been used as a measure of the elongation prior to necking in uniaxial tensile tests. However, in forming operations, the stress-state in the material is not unidirectional and thus Considère is not necessarily the best indicator of the formability of a material. Moreover, the ability of a material to resist necking can certainly be tied to the work-hardening behaviour at large-strains but upon the formation of an incipient neck, the geometry of the sample and the assumption of a uniform strain-rate break-down. The result is that an alternative approach must be considered. Observed asymmetries in precisely controlled up and down rate changes during SRS measurements in highly deformed aluminium indicated that recovery is an important factor depending on if deformation is taking place within the interior (increased strain-rate) or exterior (decreased strain-rate) of the necked region of a deformed sample (Diak and Saimoto, 1995). In the current work, the role of the engineering strain-rate sensitivity parameter, m, and thermodynamic strain-rate sensitivity, S, determined from instantaneous up-change (uc) and down-change (dc) strain-rate tests will be examined. Strain-rate sensitivity experiments determined by interrupted up and down strain rate changes, and continuous tensile testing along with differential scanning calorimetry (DSC), and Vickers hardness testing were used to characterize AA6xxx series alloys with varying levels of Cu, exposed to both PA and NA processes, and NA only. This information will give a general understanding of the influence of Cu on the mechanical properties and ultimately an approximation of the formability of this alloys series incorporating both m_{uc} and m_{dc} parameters. The paper first provides theoretical basis for the strain-rate sensitivity and its connection to formability, describes the experimental work done, followed by the results, their interpretation and conclusions.

Activation Volume and Strain-Rate Sensitivity

The use of SRS experiments is to determine the component of "reversible" deformation during plastic flow, herein referred to as the thermal component of deformation. Initially envisioned by Cottrell and Stokes (Cottrell & Stokes, 1955), the role of the thermal component of deformation has been widely studied (Diak, Upadhyaya, & Saimoto, 1998; Nabarro, 1990; Picu & Li, 2010; Saimoto, 2006) and a method to determine an understanding of the evolution of deformation obstacles during plastic flow has been developed. Traditionally interrupted tensile tests with intermittent annealing or temperature variations (Cottrell & Stokes, 1955) are used to probe this thermal component of deformation. The use of SRS testing was introduced to provide a more experimentally-viable testing method. In an analogous method to the temperature change method used by Cottrell and Stokes, SRS testing attempts to identify the effect of the energy barrier for thermal obstacles on plasticity such that

$$\dot{\epsilon} = \dot{\epsilon_0} \exp\left(-\frac{\Delta G(\sigma)}{kT}\right)$$

where $\dot{\epsilon}$ is the applied strain rate, $\dot{\epsilon_0}$ the base strain-rate, $\Delta G(\sigma)$ is the stress-dependent activation energy barrier, k is the Boltzmann constant and T the absolute temperature. The activation energy barrier describes the segment area swept during dislocation activation when a mobile dislocation overcomes an obstacle. In order to expand this equation in terms of a change in strain-rate resulting in an observable change in the applied stress, the following must hold

$$\frac{\partial \ln \dot{\epsilon}}{\partial \sigma} = \frac{\partial \ln \dot{\epsilon_0}}{\partial \sigma} - \frac{1}{kT}\frac{\partial \Delta G(\sigma)}{\partial \sigma}$$

The above can be manipulated to reveal the apparent inverse activation volume at constant temperature, T, and structure, Σ, as

$$\frac{1}{V'} = \frac{1}{kT}\frac{\partial \sigma}{\partial \ln \dot{\epsilon}}\Big|_{T,\Sigma}$$

Since the products formed during plasticity by dislocation glide are dislocation arrays, a plot of $\frac{1}{T}\frac{\Delta\sigma}{\Delta \ln \dot{\epsilon}}$ versus $(\sigma - \sigma_{0.2\%})$, referred to as the Haasen plot in the literature, captures the hardening

behaviour, where the Δ replaces the ∂ to represent a discrete experimental measurement. The slope of the Haasen plot gives the thermodynamic SRS parameter of the material as $S = \frac{1}{T}\frac{\Delta\sigma}{\sigma\,\Delta\ln\dot{\epsilon}}$, where the intercept of the Haasen plot, $\frac{1}{T}\frac{\partial\sigma}{\partial\ln\dot{\epsilon}}$, is related to the rate controlling obstacle density at yield as k/V'. Alternatively, the instantaneous engineering SRS, m_i, is determined directly from the change in the stress due to a change in the plastic strain-rate given as

$$m_i = \frac{\Delta\ln\sigma}{\Delta\ln\dot{\epsilon}}\Big|_{T,\Sigma}$$

which can be related back to the thermodynamic parameter S by m = ST. However, during deformation of age-hardenable aluminum alloys (and all aluminum alloys), the rate controlling obstacles begin as solutes, clusters and/or precipitates being either stronger or weaker than the rate controlling forest dislocation, and typically of higher densities than the initial dislocations distribution after solutionizing and ageing heat treatments. At the onset of plastic deformation, the weaker obstacles dominate the energy landscape of the alloy such that they are "rate-controlling" but as deformation progresses and dislocations multiply in order to accommodate the imposed deformation (at a rate dependent on the imposed strain-rate), the effects of these initial obstacles become obscured and the result is that dislocation-dislocation interactions dominate. It is however possible for other obstacles to be formed during deformation such as point defects, stacking fault tetrahedra, nano-voids, and dislocation debris that may also contribute to changes in the observed strain-rate sensitivity (Argon, 2008).

Strain-Rate Sensitivity Influence on Formability

Consider a Hollomon-type constitutive equation of the form

$$\sigma = \sigma_0 + K\epsilon^n\dot{\epsilon}^m$$

where σ is the flow stress, σ_0 is the proportional limit, ϵ is the current logarithmic strain, $\dot{\epsilon}$ is the current applied true strain rate, and K is a pre-exponential constant. The general form of the Considère criterion would yield

$$\frac{d\sigma}{d\epsilon} = n = \sigma$$

where $d\sigma/d\epsilon$ is the current work-hardening rate, n. If the Hollomon-type equation is differentiated with respect to strain, the relation becomes

$$\frac{d\sigma}{d\epsilon} = \frac{K\epsilon^n\dot{\epsilon}^m}{\epsilon}\left(n + m\frac{\partial\ln\dot{\epsilon}}{\partial\ln\epsilon}\right) = \sigma$$

It is clear that the term $\partial\ln\dot{\epsilon}\,/\partial\ln\epsilon$ will be zero prior to any neck formation since the deformation applied is assumed to be uniform and the traditional Considère criterion is restored. However, upon the formation of the neck, this strain-rate sensitivity component of deformation can be positive, null, or negative, which affects whether the local strain rate increases with strain (neck interior) or decreases with strain (neck exterior). The result is that the Hollomon relation, which determines the current stress-state of the local region, must be compared to that of the new, strain-rate affected work-hardening relationship to determine if the Considère criterion is still met under these new deformation conditions. Thus, the comparison of current local stress and work-hardening states interior and exterior to the neck are most important to determining the formability whereby the strain-rate sensitivity will in fact influence the total formability of the alloy upon the onset of diffuse necking.

METHODS AND MATERIALS

The materials were received in the form of 1 mm thick sheets in the as-rolled condition provided by Constellium. The alloys were all based on an AA6116 alloy composition (Al-0.35Mg-0.9Si) with either 0, 0.2, or 0.8 wt% Cu. Samples were extracted from the sheets (tensile/SRS specimen, hardness, or small coupons to be used for DSC measurements). Hardness samples were prepared using standard grinding (1200p), polishing (9 µm then 3 µm), and mechanical etching (0.05 µm silica) procedures and were then solution heat treated (SHT) at 550°C for 15 minutes; followed by water quenching (WQ), or PA at 80°C for 8 hours followed by water quenching. Samples were taken to the T4-1M condition by WQ with 1 month of NA and the T4PA-1M condition after the PA process with 1 month of subsequent NA. Hardness samples were tested immediately (within 5 minutes) of WQ to determine the baseline hardness and were given a secondary light polish with the silica etchant to remove any oxide layer formed during the SHT process. The same hardness specimen were tested in appropriate time intervals to establish the subsequent NA curves for each of the alloys in both the PA and NA-only conditions. Hardness measurements reported were taken using an automated Vickers Hardness indenter with a 100 g load and a 30 s dwell time, the average of 10 measurements being reported. DSC measurements were performed using a Mettler Toledo DSC at a heating rate of 20°C/min up to 300°C for both the WQ and 30 day NA conditions (only the 30 day NA condition is included in this paper). Tensile tests were performed on a hydraulic INSTRON instrumented with a 25 mm extensometer with ± 10 mm extension, pulled at a constant, true strain-rate of 5×10^{-4} s^{-1}, until failure for samples in the T4-1M and T4PA-1M conditions. Strain-rate sensitivity experiments were performed on the same INSTRON at a base true-strain rate of 5×10^{-4} s^{-1} with intermittent changes using the step-ramp method (Carlone & Saimoto, 1996) by a factor of 4 or 10 for up rate-changes or a factor of 1/4 or 1/10 for down rate-changes such that 10^{-4} to 10^{-3} s^{-1} measures m_{uc} or S_{uc}, and 10^{-4} to 10^{-5} s^{-1} measures m_{dc} or S_{dc}.

RESULTS AND ANALYSIS

Understanding the effects of Cu on NA behaviour and the corresponding cluster formation may be aided through analysis of the NA hardness curves, Figures 1a and 1b, and the corresponding DSC scans of formed products after 30 days NA, Figure 2a, compared to those formed during the PA process, Figure 2b.

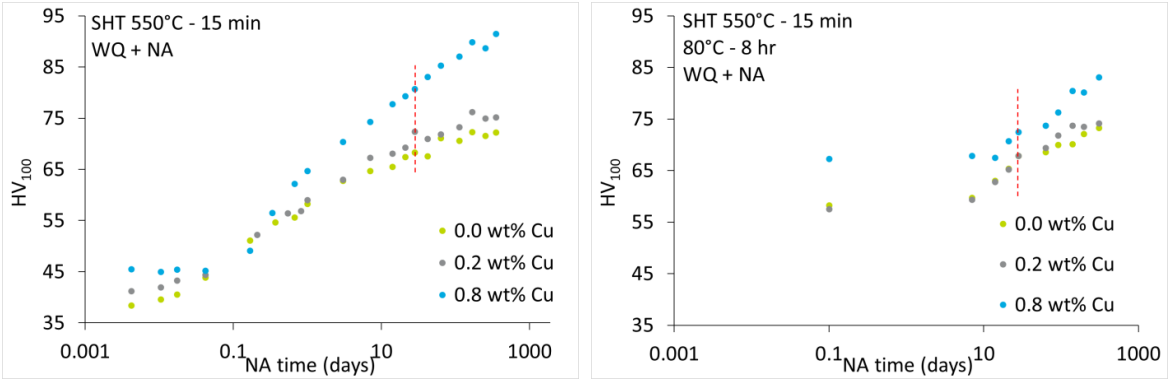

Figure 1. NA Vickers hardness curves for the three alloys studied after a) solutionizing at 550°C for 15 minutes, WQ and NA, and b) after SHT at 550°C for 15 minutes, directly PA at 80°C for 8 hours and finally WQ, then NA. Each point is the average of 10 indents on a single sample. Scatter in measurements was typically ± 1 HV_{100}. The dashed vertical line indicates 30 days of NA for the WQ and WQ + PA samples.

The addition of Cu was found to increase the initial and final hardness values in both the WQ and PA conditions. However, the addition of 0.2 wt% Cu does not appear to significantly influence the hardness in the PA condition. It is interesting to note that the difference in hardness in the T4-1M condition is greater than that of the T4PA-1M condition with increased Cu. The nature of the clusters formed during

the NA and PA processes and the subsequent precipitation are evidenced by the DSC scans in Figures 2a and 2b, respectively.

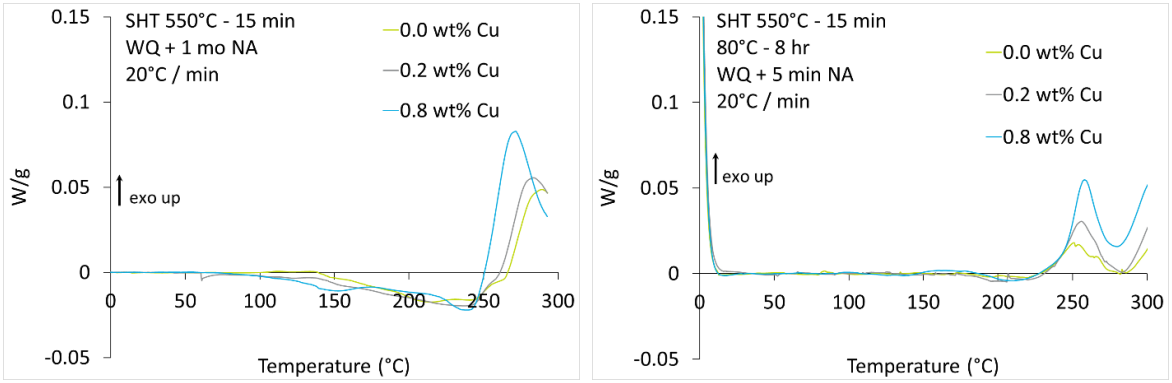

Figure 2. a) DSC scans for the three alloys studied in a) T4-1M, and b) PA + WQ (T4PA-0M) conditions.

In the T4-1M condition, two distinct clusters dissolution peaks can be observed occurring at 150°C and 230°C, the first one being increasingly visible with increasing Cu content. An addition of Cu translates into a greater precipitation signal occurring at lower temperature (260°C vs. 300°C), consistent with a decrease in the negative natural ageing effect with additions of Cu. In the T4PA-0M condition, the clusters present in the microstructure appear to be more stable, since only a very limited dissolution peak is observed around 200°C, independent of Cu content. Yet, again the addition of Cu strongly enhances the precipitation signal around 260°C, with only minor changes in the peak temperature, contrary to the NA case. It is interesting to note that the precipitation peak temperature in the T4PA-0M condition is lower that of the T4-1M condition suggesting that the clusters formed during the PA process are closer in stoichiometric ratio to the precipitates formed during the PB cycle, consistent with the use of PA to enhance the PB response in this alloy series. Additionally, the relative difference in precipitation peak temperature for each of the alloys decreases with Cu content when comparing the T4-1M and T4PA-0M treatments – that is to say, Cu addition may reduce the need to apply the PA treatment compared to the Cu-free alloys. The discrepancies between the clusters formed under the two heat treatment conditions become apparent when observing their continuous deformation behaviour shown in Figures 3a and 3b.

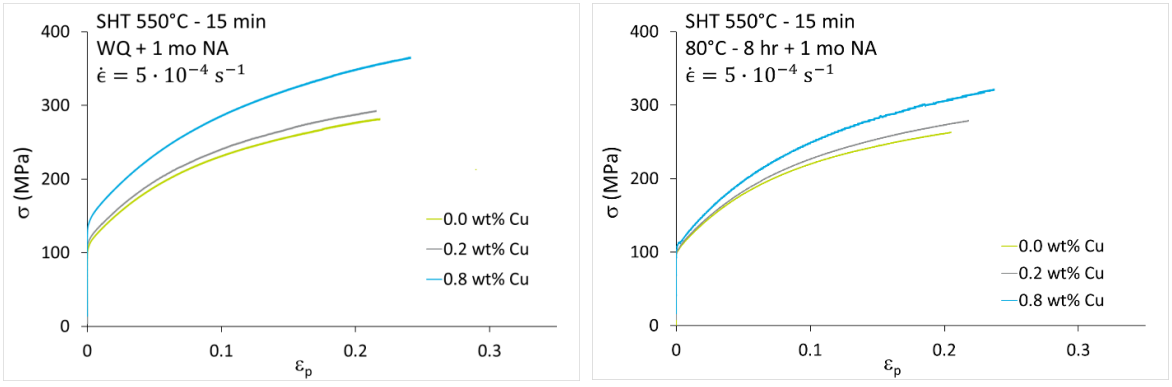

Figure 3. True stress versus true plastic strain curves for the three alloys tested in the a) T4-1M, and b) T4PA-1M conditions at room temperature with a constant true strain rate of $5 \times 10^{-4}\ s^{-1}$.

The yield stress of the alloys in the T4-1M condition are significantly increased with Cu but this effect is absent in the T4PA-1M treatment with the exception of an introduction of a yield point effect within the 0.8 wt% Cu alloy. It is interesting to note that the ultimate tensile stress (UTS) is increased in

both of the heat treatment series due to Cu additions. A full tabulation of the mechanical properties are presented in Table 1.

Table 1. Summary of the mechanical properties for each of the alloys tested either during continuous tensile tests or SRS tests. *The sample failed at the knife-edge of the extensometer

Cu content (wt %)	Condition	$\sigma_{0.2\%}$ (MPa)	UTS (MPa)	UTS - $\sigma_{0.2\%}$ (MPa)	n = ε_L
0.0	T4-1M	113	282	169	0.219
0.2		119	292	173	0.212*
0.8		144	365	221	0.241
0.0	T4PA-1M	104	262	159	0.204
0.2		105	278	173	0.217
0.8		112	319	207	0.235

There is an onset of flow instabilities in the 0.8 wt% Cu alloy at 0.14 strain, consistent with the appearance of the yield point in the T4PA-1M condition. The addition of Cu appears to increase the uniform elongation until reaching the Considère criterion (the 0.2 wt% Cu T4 sample failed on the knife edge of the extensometer) consistent with the increased work-hardening observed as shown in Figures 4a and 4b. However, it should also be noted that the relative elongation to failure between alloys in T4-1M and T4PA-1M were not appreciably different consistent with the T4-1M condition having a similar work-hardening capacity compared to the T4PA-1M state.

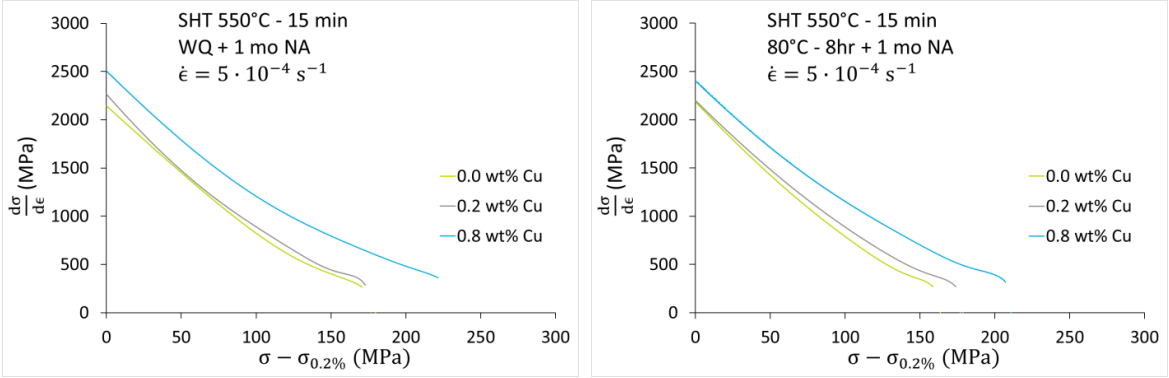

Figure 4. Kocks-Mecking plots of Figs. 3 showing work hardening rate versus corrected stress for the three alloys tested in the a) T4-1M, and b) T4PA-1M conditions.

The initial work-hardening rate in the T4-1M condition was found to increase with Cu to a greater extent than that of T4PA-1M condition. However, the recovery behaviour appeared to be more effected due to Cu additions in the T4PA-1M condition whereby the additional Cu aided in retarding dislocation recovery during deformation, possibly due to the presence of additional solute remaining in solution. For both heat treatments, drastic increases in the initial work-hardening coupled with retarded recovery result in enhanced elongation prior to failure seen most predominantly in the 0.8 wt% Cu alloy. How the work-hardening and cluster presence relates to the thermodynamic SRS of these alloys under the two conditions are shown in the Haasen plots below in Figures 5a and 5b.

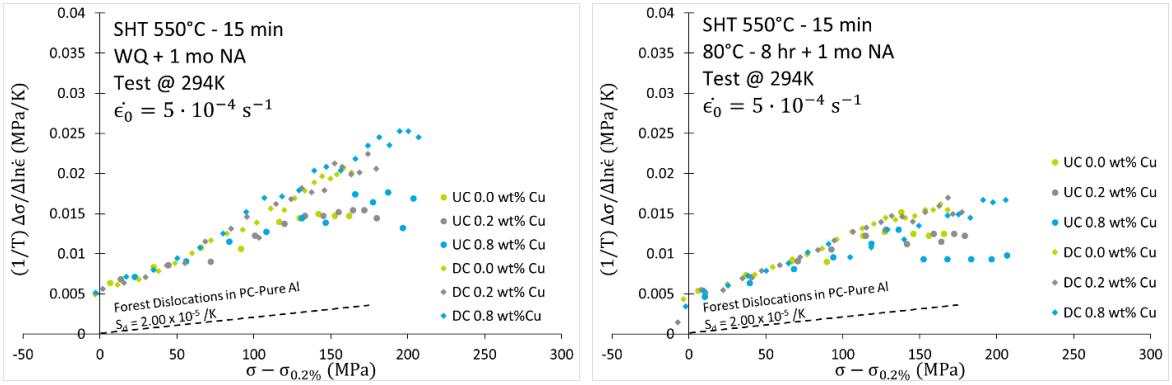

Figure 5. Haasen plots for the three alloys tested in the a) T4-1M and b) T4PA-1M conditions for both up-changes (UC, circles) and down-changes (DC, diamonds) tested at room temperature. The forest dislocation lines for pure poly-crystal aluminum are shown for comparison (B. J. Diak et al., 1998), for clarity the forest dislocation line has been ended early.

Several observations can be easily made from the Haasen plots in Figure 5 and the values summarized in Table 2: (1) the measured curves have values larger than the pure metal line; (2) the measured curves are initially quite linear, but with slopes larger than the forest dislocation line; (3) the T4-1M conditions for all alloys exceed the maximum value and display higher SRS values than their T4PA-1M counterparts; (4) there appears to be a significant drop in the stress change at some critical stress in the T4PA-1M condition; and (5) there is no measureable difference in the up-change and down-change values at stresses just above the yield stress, but they diverge after work-hardening of about 50–100 MPa. It can also be seen that the initial SRS (slope of the Haasen plot) directly after yield is considerably lower than after substantial work-hardening in the T4-1M alloys, this suggests that the initial obstacles formed in this heat treatment are more easily thermally activated than the mobile dislocations produced in this alloy. The influence of Cu in the T4PA-1M condition appears to be lesser than that in the T4-1M condition likely due to the presence of two cluster types in T4-1M that are absent in T4PA-1M (see the two distinct dissolution peaks in Figure 2a which is absent in Figure 2b). However, the Cu additions in the T4PA-1M decreased the absolute values at large flow stresses, attributed to the presence of serrated flow during deformation.

Table 2. The SRS properties of the three alloys testing in the two heat treatment conditions at yield ($\sigma_{0.2\%}$) and Considère strain (ε_L).

Cu content (wt %)	**Condition**	**S_{dc} ($\sigma_{0.2\%}$) $\times 10^{-5}$ (K^{-1})**	**S_{uc} ($\sigma_{0.2\%}$) $\times 10^{-5}$ (K^{-1})**	**S_{dc} (ε_L) $\times 10^{-5}$ (K^{-1})**	**S_{uc} (ε_L) $\times 10^{-5}$ (K^{-1})**
0.0		6.7	6.3	12.4	2.3
0.2	T4-1M	6.8	6.4	11.0	2.3
0.8		7.0	6.8	10.4	1.7
0.0		5.1	4.6	8.4	–0.5
0.2	T4PA-1M	5.2	6.5	8.2	–0.3
0.8		6.4	5.9	6.8	0.0

Cu content (wt %)	**Condition**	**S_{dc} ($\sigma_{0.2\%}$)T**	**S_{uc} ($\sigma_{0.2\%}$)T**	**S_{dc} (ε_L)T**	**S_{uc} (ε_L)T**	**m_{dc} (ε_L)**	**m_{uc} (ε_L)**
0.0		0.020	0.019	0.037	0.007	0.022	0.017
0.2	T4-1M	0.020	0.019	0.033	0.007	0.022	0.016
0.8		0.021	0.020	0.031	0.005	0.022	0.015
0.0		0.015	0.014	0.025	–0.002	0.018	0.014
0.2	T4PA-1M	0.015	0.019	0.024	–0.001	0.017	0.013
0.8		0.019	0.018	0.020	0.000	0.016	0.010

In parallel, the engineering SRS values, m_i, for these alloys and conditions are shown above in Figures 6a and 6b. The same observations may be made for the engineering SRS values compared to the thermodynamic SRS. The initial $S_{uc}T$ and $S_{dc}T$ (at $\sigma_{0.2\%}$) values do not vary significantly between the T4-1M and T4PA-1M (see Table 2) conditions, but appear to increase with Cu content, while all m-values remain greater than those for forest dislocations in pure poly-crystalline aluminium. The T4-1M condition m-values monotonically increase during deformation up until very large flow stresses (80~90% max stress) whereas the T4PA-1M values show a sudden decrease (around 150 MPa) suspected to be related to the onset of flow instabilities during deformation. The peak m_{uc} and m_{dc} values are consistently greater for the T4-1M condition compared to the alloys in the T4PA-1M conditions. The differences and importance of the up-change and down-change values are discussed below.

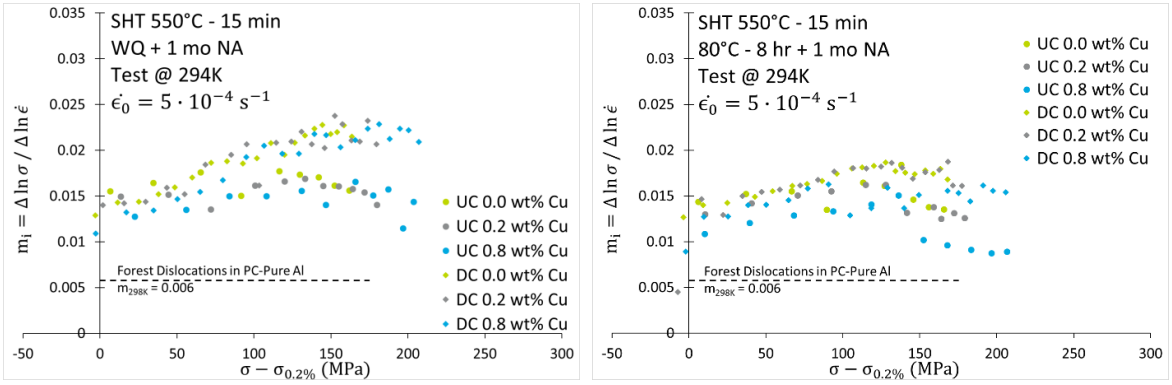

Figure 6. Engineering SRS versus corrected stress plots for both up-changes (UC, circles) and down-changes (DC, diamonds) for the three alloys tested in the a) T4-1M, and b) T4PA-1M conditions tested at room temperature.

DISCUSSION

Connecting the alloy composition and thermal treatments to the observed mechanical properties and SRS values requires extensive knowledge of the alloy systems. As such, a proposed relation will be presented for both cases of NA and PA, with extensions of the suspected role of SRS on the formability of AA6xxx series alloy sheets.

Natural Ageing: Microstructure and Resulting Properties

As first noticed in the DSC signature with Cu additions, the presence of a low-temperature dissolution peak was less pronounced in the Cu-free alloy and appears to be related to additional less-thermally stable clusters being formed. Aruga et al. (Aruga, Kozuka, Takaki, & Sato, 2015) noted that the cluster type i formed at ambient temperatures appeared to be more thermodynamically stable than those of type ii, despite being formed at lower temperatures. As such, it is not surprising that the existence of this dissolution peak would be more predominant in the high-Cu alloys likely having a (Cu + Mg)/Si ratio greater than the low-Cu alloys. Based on the total solute content and the likelihood of having a greater number density of clusters and/or size in these alloys, it is no surprise that the yield strength is strongly enhanced with the additional Cu. The reduction in dislocation recovery during deformation is possibly due to the secondary, type i clusters, acting in a similar nature to solute atoms but with a reduced mobility. If the larger, type ii clusters are the main thermal obstacles being overcome during deformation then the SRS of the material should be dictated by them at yield. Thus it would be expected that the intercept and initial SRS should be greater, having an increased activation distance, which appears to be the case with added Cu.

Pre-Ageing: Microstructure and Resulting Properties

Unlike the alloys in the T4-1M condition, the DSC signatures appear less affected by the additions of Cu such that there is no secondary cluster dissolution in the T4PA-0M condition. This extends to the yield strengths each of the alloys being almost identical and the appearance of a yield point effect in the high-Cu alloy possibly due to the retention and growth of clusters formed during the subsequent NA process after the PA treatment (see the small exothermic peak in Figure 2b). Although only based on speculation, if solutes are retained in solution and/or clusters mechanically dissolved being cut/sheared by dislocations, it would correlate with the onset of flow instabilities observed in the higher-Cu content alloys and the deviations from a monotonically increasing Haasen plot occurring at lower flow stress with increasing Cu content (see figure 5b). This mechanism would be coupled with the retardation of dislocation recovery and sustained work-hardening observed in the higher-Cu alloys whereby the dislocations may be stabilized through the added "friction" caused by dynamic dislocation-solute atom interactions on the glide plane. The coupling of these effects would yield to an increased uniform elongation with Cu additions, as observed.

Connecting Strain-Rate Sensitivity to Formability: The Asymmetry of Rate-Changes

The current results are the first quantitative observation of a flow stress asymmetry in the Al-Mg-Si-Cu alloy system due to increasing or decreasing strain rate. The asymmetry has been related to the temperature dependent short-range annihilation of small debris (dislocations, point defects, small dislocation loops, etc.) in nominally pure aluminum alloys occurring on a very short time scale (Diak & Saimoto, 1995; Saimoto & Duesbery, 1984) resulting in additional stress decreases during the rate change causing the apparent SRS to be increased ($S \sim \Delta \ln \sigma$). Recovery is only possible for down-change tests after larger strains due to the surplus dislocation density available at the "steady-state" production rate (base strain-rate) resulting in the recovery of debris that is not required during the instantaneous increase in strain rate. This effect is clearly evident in both the thermodynamic SRS values, $S_{dc}T$ and $S_{uc}T$ at ε_L whereby up-change values are substantially lower showing a very large discrepancy. The onset and incubation stress (work hardened state) required prior to the separation of up-change and down-change tests depends on both the testing temperature and the cluster/precipitate state of the material influencing the production of debris products. It is interesting to note that in the T4PA-1M condition, the $S_{uc}T$ terms are negative or zero at high strain, unlike the m_{uc} values which are low but still positive. This is due to the definition of the value of S from the Haasen plot whereby the rate of change of the stress drop ($\Delta\sigma$) is more important than the physical value ($\Delta \ln \sigma$) as calculated for m. For this reason, evolutions of the thermodynamic SRS are better used for advanced modelling incorporating the relative contributions of clusters, dislocations, and debris, on the total SRS response of the alloy during deformation. It would appear from this work that the additional Cu reduces the recovery of debris (or produces less debris) based on the differences between; $S_{uc}T$ and $S_{dc}T$ at large strains, decreasing with Cu content. However, the differences in these values are not solely responsible for the delay of necking in AA6xxx series alloys as both the m_{uc} and m_{dc} both affect the stress states for the interior and exterior of the necked region, respectively. As such it is necessary to study and use both of these values when modeling neck formation is both uniaxial tensile tests as well as formability tests.

CONCLUSIONS

The following conclusions can be made from this work:

- Cu appears to have an influence on the clustering response in the T4 condition resulting in an augmented hardness, yield strength, and UTS of the alloys. When the alloys are pre-aged before natural ageing as in the T4PA-1M condition, the yield strength effects are strongly reduced (increase of only 9% compared to 27% for T4-1M) while the hardness and UTS effects of Cu addition remain.
- Additional Cu is shown to increase the work-hardening capacity and retard dislocation recovery during deformation resulting in an enhanced total uniform elongation for both T4-1M and T4PA-1M conditions.

- The engineering SRS for both m_{uc} and m_{dc} were found to decrease with Cu content for both heat treatments with the T4-1M condition showing superior SRS compared to T4PA-1M.
- The asymmetry in the m_{uc} and m_{dc}, and their absolute values are both important for the study of necking formation as both components affect the local stress states and thus the Considère criterion; this phenomenon should be further explored.

ACKNOWLEDGMENTS

The author would like to thank the Association Nationale Recherche Technologie (ANRT) for co-funding the project and Devang Sejani for performing the extensive hardness testing found in this work.

REFERENCES

Argon, A. S. (2008). *Strengthening Mechanisms in Crystal Plasticity*, Oxford University Press.

Aruga, Y., Kozuka, M., Takaki, Y., & Sato, T. (2015). Formation and reversion of clusters during natural aging and subsequent artificial aging in an Al–Mg–Si alloy. *Materials Science and Engineering: A*, *631*, 86–96. https://doi.org/10.1016/j.msea.2015.02.035

Carlone, M., & Saimoto, S. (1996). Precision strain rate sensitivity measurement using the step-ramp method. *Experimental Mechanics*, *36*(4), 360–366.

Cottrell, A. H., & Stokes, R. J. (1955). Effects of Temperature on the Plastic Properties of Aluminium Crystals. *Proceedings of the Royal Society A: Mathematical, Physical and Engineering Sciences*, *233*(1192), 17–34. https://doi.org/10.1098/rspa.1955.0243

Diak, B. J. & Saimoto, S. (1995). Role of Strain Rate Sensitivity on Diffuse Necking, in Plasticity '95, suppl. vol. (Eds. Tanimura and Khan) pp.5-9.

Diak, B. J., Upadhyaya, K. R., & Saimoto, S. (1998). Characterization of thermodynamic response by materials testing. *Progress in Materials Science*, *43*(4), 223–363.

Esmaeili, S., Wang, X., Lloyd, D. J., & Poole, W. J. (2003). On the precipitation-hardening behavior of the Al-Mg-Si-Cu alloy AA6111. *Metallurgical and Materials Transactions A*, *34*(3), 751–763.

Hirsch, J. (2004). Automotive trends in aluminium-The European perspective. In *Materials Forum* (Vol. 28, pp. 15–23). Retrieved from https://www.researchgate.net/profile/Juergen_Hirsch/publication/242553245_Automotive_Trends_in_Aluminium_-_The_European_Perspective/links/0deec52c69d5f1fef9000000.pdf

Hirsch, J. (2014). Recent development in aluminium for automotive applications. *Transactions of Nonferrous Metals Society of China*, *24*(7), 1995–2002. https://doi.org/10.1016/S1003-6326(14)63305-7

Kim, J. H., & Sato, T. (2011). Effects of Cu Addition on Nanocluster Formation and Two-Step Aging Behaviors of Al–Mg–Si Alloys. *Journal of Nanoscience and Nanotechnology*, *11*(2), 1319–1322. https://doi.org/10.1166/jnn.2011.3344

Murayama, M., & Hono, K. (1999). Pre-precipitate clusters and precipitation processes in Al–Mg–Si alloys. *Acta Materialia*, *47*(5), 1537–1548.

Murayama, M., Hono, K., Miao, W. F., & Laughlin, D. E. (2001). The effect of Cu additions on the precipitation kinetics in an Al-Mg-Si alloy with excess Si. *Metallurgical and Materials Transactions A*, *32*(2), 239–246.

Nabarro, F. R. N. (1990). Cottrell-Stokes law and activation theory. *Acta Metallurgica et Materialia*, *38*(2), 161–164.

Picu, R. C., & Li, R. (2010). On the relationship between the Cottrell–Stokes law and the Haasen plot. *Materials Science and Engineering: A*, *527*(20), 5303–5306. https://doi.org/10.1016/j.msea.2010.04.093

Saimoto, S. (2006). Dynamic dislocation–defect analysis. *Philosophical Magazine*, *86*(27), 4213–4233. https://doi.org/10.1080/14786430500367347

Saimoto, S., & Duesbery, M. S. (1984). Strain rate sensitivity: the role of dislocation loop and point defect recovery. *Acta Metallurgica*, *32*(1), 147–155.

Tao, G. H., Liu, C. H., Chen, J. H., Lai, Y. X., Ma, P. P., & Liu, L. M. (2015). The influence of Mg/Si ratio on the negative natural aging effect in Al–Mg–Si–Cu alloys. *Materials Science and Engineering: A*, *642*, 241–248. https://doi.org/10.1016/j.msea.2015.06.090

Wenner, S., Marioara, C. D., Andersen, S. J., & Holmestad, R. (2012). Effect of room temperature storage time on precipitation in Al–Mg–Si (–Cu) alloys with different Mg/Si ratios. *International Journal of Materials Research*, *103*(8), 948–954.